Landsat TM-Based Forest Damage Assessment: Correction for Topographic Effects

Sam Ekstrand

Abstract

Detection of forest damage is one of the various remote sensing applications complicated by topographic effects. Different vegetation types are known to respond differently to slope and illumination effects. This paper describes the response of Landsat Thematic Mapper data to the topography in Norway spruce forest, and the possibility to assess forest damage in rugged terrain. The effect at the examined medium and low solar elevations was non-Lambertian. Minnaert corrections and other empirical functions proposed for different cover types were found to be inadequate. Two new models were developed; one based on Minnaert constants changing with the cosine of the incidence angle, and the other based on an empirical relationship. Both models gave satisfactory results although the empirical model performed better for nearly shadowed northern slopes. With a model accounting for terrain and canopy inhomogeneity effects using digitized stand data and digital elevation models, healthy to slightly defoliated spruce forest could be separated from moderately defoliated forest. The method enables an improvement of the earlier documented Landsat TM capability to detect severely damaged forest.

Introduction

The operational use of remote sensing techniques is often obstructed by problems originating from topographic effects on the sensor response. Forest damage assessment is one of the applications complicated by such problems. Earlier satellite studies have suggested that Landsat TM is capable of mapping severe forest damage (Ciolkosz and Zawila-Niedzwiecki, 1990; Rock *et al.*, 1986; Vogelmann, 1990). Techniques enabling monitoring of moderate damage are also of principal interest, because they strongly facilitate management actions aiming to prevent production losses and the evolving of irreversible damage. The capability to detect slight or moderate forest decline with satellite and airborne data has been found to be very sensitive to natural variations in stand characteristics and terrain (Ekstrand, 1990; Ekstrand, 1994a; Leckie, 1987; Westman and Price, 1988). However, when using a model employing stand data from digitized forest maps to account for variations in stand age, species composition, and density, it has been possible to distinguish between healthy and moderately defoliated spruce forest on horizontal ground using Landsat TM (Ekstrand, 1994a). To make the method feasible over larger areas, it is also necessary to be able to correct for topographic effects.

Apart from irradiance variations due to atmospheric optical properties, the irradiance received by the target varies with the cosine of the incidence angle. Due to atmospheric scattering, the sun elevation is also of importance. A surface perpendicular to the sun at a low sun elevation will receive less radiation than a surface perpendicular to the sun at a high solar elevation. To some extent, the incoming radiation also varies with the target altitude because the optical thickness of the atmosphere decreases at higher altitudes (Yugui, 1989). The amount of reflected radiation from the target depends on the class-specific reflection in different directions described by the bidirectional reflectance function (e.g., Kriebel, 1976). It also depends on whether the geometric structure of the forest type changes with slope. According to Kimes and Kirchner (1981), there is a need for measurements on a large number of vegetation types on inclined surfaces. Measurements of topographic effects have demonstrated that different types of vegetation respond differently to direction and illumination effects (Holben and Justice, 1980; Leprieur *et al.*, 1988; Thomson and Jones, 1990). In agreement with this, Teillet *et al.* (1982) found that slope-aspect corrections in forestry applications must be class-specific and that no correction formula is sufficiently general to accommodate the various forest types. Syrén (1991) found that the vertical canopy structure of different species strongly influences the rate at which reflectance decreases as a function of decreasing sun elevation. This indicates that the spectral response to an increasing angle between the surface normal and the solar beam due to topography is also dependent on vertical canopy structure.

The use of ratio algorithms has been reported to partly resolve the problem of variable illumination, provided that the atmospheric path radiance term is eliminated (Kowalik *et al.*, 1983; Chavez and Mitchell, 1977; Rowan *et al.*, 1977). The method has been used to detect severe forest decline in areas suffering from both defoliation and chlorosis symptoms (Rock *et al.*, 1986; Rosengren and Ekstrand, 1987; Vogelmann, 1990). Chlorosis is defined as a persistent yellow discoloration on the sun-exposed upper side of the branches. However, in areas with moderate defoliation and no chlorosis, Ekstrand (1994a) found that ratios gave inferior results compared to a near-infrared single band variable due to poor correlation with moderate defoliation in the visible and shortwave infrared (SWIR) bands. These results support the findings of Koch *et al.* (1990) who also presented poor relationships between defoliation and visible and SWIR spectral bands. The only consistent spectral effect of defoliation was a decrease in the near infrared spectral band. This implied that an empirical correction based on digital slope/aspect data would be more appropriate than a ratio correction for the application considered here. Both methods are investigated in this paper.

The purpose of the project was to develop a method for correction of topographic effects in spruce forest, to incorpo-

Swedish Environmental Research Institute, Box 21060, S-100 31 Stockholm, Sweden.

Photogrammetric Engineering & Remote Sensing, Vol. 62, No. 2, February 1996, pp. 151–161.

0099-1112/96/6202-151$3.00/0

rate the method in the defoliation assessment model and to determine the operational accuracy of the defoliation estimation.

Lambertian and Non-Lambertian Models

A Lambertian surface is presumed to be a perfectly diffuse reflector, appearing equally bright from all viewing directions. Therefore, a Lambertian correction function attempts to correct only for differences in illumination caused by the orientation of the surface (Jones *et al.*, 1988). Radiance is assumed to be proportional to the cosine of the incident angle. The incidence angle (i) is the angle between the surface normal and the solar beam, and may be calculated by (Smith *et al.*, 1980; Holben and Justice, 1980)

$$\cos i = \cos e \cos z + \sin e \sin z \cos(\phi_s - \phi_n), \quad (1)$$

where e = surface normal zenith angle or terrain slope,
z = solar zenith angle,
ϕ_s = solar azimuth angle, and
ϕ_n = surface aspect of the slope angle.

Northern slopes approaching the point where the surface is in shadow ($\cos i < 0$) should, according to the Lambertian assumption, have no reflectance. However, during daytime, diffuse sky irradiance will always reach the surface, and part of it will be reflected. It may be advocated that the surface itself may still be nearly Lambertian but, as seen from the satellite, it is not. Several authors have found that the sky irradiation cannot be neglected for pixels with low direct illumination (e.g., Proy *et al.*, 1989; Kimes and Kirchner, 1981), and that non-Lambertian assumptions provide superior results for vegetated surfaces (Colby, 1991; Jones *et al.*, 1988; Leprieur *et al.*, 1988; Smith *et al.*, 1980; Teillet *et al.*, 1982, Thomson and Jones, 1990; Woodham and Grey, 1987). However, both sand (Holben and Justice, 1980) and forested surfaces (Cavayas, 1987; Smith *et al.*, 1980; Teillet *et al.*, 1982) have been found to be nearly Lambertian at high solar elevations when the effective incidence angle is relatively low, including the incidence angles for northern slopes. Kawata *et al.* (1988) attributed the rejection of the Lambertian model by previous researchers to a presumed incorrect use of digital terrain data. However, several of the authors above did not use digital terrain data for the determination of slope/aspect in the test sites (e.g., Holben and Justice, 1980; Smith *et al.*, 1980; Thomson and Jones, 1990). If atmospheric path radiance is removed in advance and sky irradiance is neglected, the Lambertian cosine correction is (Smith *et al.*, 1980)

$$Ln(\lambda) = L(\lambda)/\cos i, \quad (2)$$

where $Ln(\lambda)$ is the effective normal response that would be measured when the incidence and slope angles both are at zero, i.e., when the surface is perpendicular to a sun in zenith. When the sun is not in zenith, correction of the radiance of an inclined surface to the radiance of a projected horizontal surface would be achieved by the function (Teillet *et al.*, 1982)

$$L_H(\lambda) = L_T(\lambda) \cos z/\cos i, \quad (3)$$

where $L_H(\lambda)$ is the radiance for a horizontal surface and $L_T(\lambda)$ is the radiance observed over the inclined terrain.

As mentioned, the majority of previous works have shown that this correction is inappropriate for forest vegetation, with an exception of high solar elevations. The model generally causes over-correction of northern slopes. The most common way to account for the non-Lambertian behavior of vegetation has been to employ the Minnaert constant (Colby, 1991; Jones *et al.*, 1988; Smith *et al.*, 1980; Teillet *et al.*, 1982; Woodham and Grey, 1987). This function was originally proposed for lunar applications by Minnaert (1941), in which the constant k was used to describe the surface roughness. In the study by Smith *et al.* (1980), the function was used to give the satellite radiance by

$$L(\lambda,e) = Ln(\lambda)\cos^{k(\lambda)} i \cos^{k(\lambda)-1} e, \quad (4)$$

where k is the Minnaert constant. The constant can be derived by first linearizing Equation 4. Then obtaining the regression value for k, using (Smith *et al.*, 1980; Colby, 1991),

$$L \cos e = Ln \cos^k i \cos^k e,$$

and

$$\log (L \cos e) = \log Ln + k \log (\cos i \cos e),$$

where $y = \log (L \cos e)$, the response variable;
$x = \log (\cos i \cos e)$, the independent variable; and
$b = \log (ln)$,
the linear form, is obtained from $y = kx + b$. The equation is then solved for k, the Minnaert constant. However, this approach requires data on Ln, the radiance for spruce forest when $i = e = 0$, that is, for horizontal surfaces *when the sun is in zenith*. Such data were not available for the present study. However, Equation 4 may be inverted to develop a Minnaert backwards radiance correction for topographic slope and aspect (Smith *et al.*, 1980; Colby, 1991): i.e.,

$$Ln = L (\cos e/(\cos^k i \cos^k e)). \quad (5)$$

Correction of the radiance over an inclined surface to the radiance over a projected horizontal surface when the solar zenith angle diverges from zero, is achieved by the relationship

$$L_H = L_T ((\cos e \cos^k z)/(\cos^k i \cos^k e)), \quad (6)$$

where $\cos^k z$ accounts for the fact that the sun is not in zenith. An alternative approach to the linearization of Equation 4 is to calculate the value for k by resolving Equation 6 for k. This was possible because the radiance of horizontal surfaces (L_H) was known, as well as the radiance of inclined surfaces (L_T).

Other empirical or semi-empirical functions have been presented by, for example, Civco (1989), Teillet *et al.* (1982), and Tomppo (1989). They generally use constants to modify the dependence on cos i, or to further adjust the effect of the Minnaert constant (k).

The causes of the non-Lambertian behavior of the different forest types are still to be clarified. Information gaps exist regarding the relative significance of sky irradiance, class-specific reflection in different directions, and variations in the geometric canopy structure. However, empirical functions like the Minnaert equation do not require such knowledge and may therefore be the only corrections applicable for the time being.

Most of the above "Minnaert papers" showed that the k value, or the degree of non-Lambertian behavior, is wavelength dependent and, consequently, presented one value for each spectral band. The main reason for the divergent behavior of vegetation in the different wavelength bands can be traced back to the diverging amount of sky irradiance in the different spectral bands, to the wavelength dependent scattering of light by atmospheric water vapor, aerosols, etc., and to the specific reflectance characteristics of the canopy, the leaves, the branches, and the field layer background.

The tree species examined so far concerning the effect of topography as recorded by satellite are Ponderosa pine (Smith *et al.*, 1980), Lodgepole pine, and Douglas fir (Teillet *et al.*, 1982). Several authors have studied coniferous or deciduous forest, with a number of species pooled in their main classes (Cavayas, 1987; Leprieur *et al.*, 1988; Civco, 1989).

Methodology

Study Area

A forest region in the county of Bohuslän in southwestern Sweden was selected for study (Figure 1). The 300-km² area is characterized by hilly terrain with slopes of 0 to 40 degrees, although the local altitude differences are not very large, usually not more than 100 metres. The minimum altitude is zero metres (sea level) and the maximum is 196 metres. Between the hillocks are flat, fine-grained sediments. Although the forest damage symptoms are light to moderate compared to the symptoms in some parts of central Europe, Bohuslän suffers from the highest levels of damage in Sweden. The main visible symptom is defoliation (needle loss) in the upper half of the crown. The most affected stands have a mean needle loss of approximately 35 to 40 percent, with 5 to 10 percent of the trees being dead or dying. The comparatively high defoliation levels in the area are attributed to long distance air pollutants together with local emissions of sulphur dioxides, nitrogen oxides, and hydrocarbons.

The area is dominated by stands of Norway spruce (*Picea abies*), sometimes with large components of Scotch Pine (*Pinus Sylvestris*) and hardwood species such as birch (*Betula verrucosa* and *Betula pubescens*) and oak (*Quercus robur*). The forest is divided into stands of uniform age and species composition. These are well managed, and the distribution of trees within each stand is also relatively uniform. The stand size is generally 2 to 10 ha, although some stands are as small as 0.3 ha.

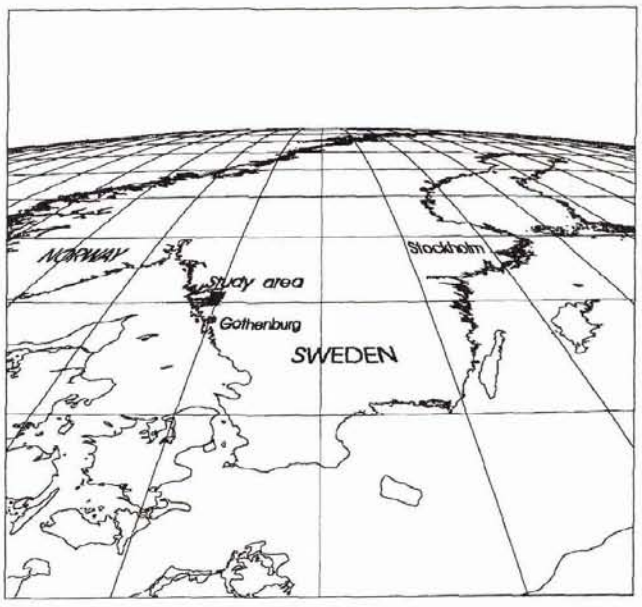

Figure 1. Location of the study area, 15 by 20 km in area (300 km²)

Preprocessing of Satellite Data

Image processing was conducted using PCI Easi/pace software and an Ebba II image processing system on personal computers. Erdas software was tested for the calculation of slope and aspect. The dates of the digital Landsat-5 TM scenes used were

- 29 August 1989, sun elevation 38°, sun azimuth 152°
- 12 September 1985, sun elevation 33°, sun azimuth 156°
- 28 September 1985, sun elevation 28°, sun azimuth 158°

Dark-lake pixel subtractions were applied to all spectral bands in order to eliminate the path radiance term, as suggested by authors referred to above (e.g., Kowalik *et al.*, 1983; Chavez and Mitchell, 1977), thereby reducing the atmospheric influence on the ratios. The water radiances in TM bands 1 through 3 were corrected to 1.23, 0.72, and 0.12 mW/(sr cm² μm), respectively, and in TM bands 4, 5, and 7 to 0, according to results presented by Bukata *et al.* (1983) for water with very small concentrations of suspended sediment and phytoplankton. These characteristics are assumed to be similar to the conditions in the lakes used for calibration. The values are also close to the clear ocean water radiance presented by Gordon (1987). The data from 1989 were geometrically precision corrected and resampled to 25-metre pixels using the standard procedure of the Swedish Landsat distributor, SSC Satellitbild, Kiruna (RMSE < 0.5 pixels). The precision correction is based on ground control points, and the resampling technique involves a cubic convolution modified to take account of the differently sized scan gaps of Landsat TM. Reduction of the pixel size is performed to retain the pixel information through the rotation procedure. It also results in a better fit of the data to the Swedish coordinate system (Westin, personal communication, 1993). The two scenes from 1985 were purchased system-corrected, and were resampled and registered to the 1989 imagery using in-house software. Late summer Landsat TM scenes were chosen because earlier results within this project indicated that spruce defoliation gives a more distinct response in late summer than in mid summer imagery (Ekstrand, 1990).

After the topographic analyses and corrections but before the final damage assessment, the scenes from 1985 were relative calibrated to the 1989 scene using a regression function derived by plotting 1985 digital counts from young forest areas against 1989 digital counts. The coefficient of determination (R^2) for TM 4 was 85.2 and the RMSE was 0.46 mW/(cm² sr μm). The resulting regression equation was used to convert 1985 data into values comparable to 1989 values (Vogelmann and Rock, 1989). Young forest areas were used because no spectrally stable ground features of sufficient size were found within the satellite scene. Furthermore, Olsson (1993) found that regression functions computed from forest pixels performed better than regression functions based on dark and bright areas (water and gravel pits) or on all types of land-cover classes. Old forest was excluded from the regression because any large scale inter-annual spectral changes caused by forest damage would otherwise have been lost in the calibration (only old trees were damaged in the area). No management actions were carried out in the young regression stands between 1985 and 1989. Therefore, there was no spectral change other than the negligible effect of four years of aging, and the possible small effects of changes in understory, lichens, amount of cones, etc. The calibration stands included bright, 20-year-old hardwood forest and darker, 50-year-old spruce. A drawback with the traditional regression method is that light areas will be underestimated and dark areas will be overestimated. This is caused by the fact that the traditional regression line of Y on X does not run through the midst of the regression points towards the ends of the point cluster. If measurement errors exist in both X and Y, the traditional method will yield biased estimates (Curran and Hay, 1986). To reduce this effect, an intermediate regression line was calculated using Wald's method instead of the traditional regression line computation. This method fits the regression line by dividing the observations into two halves on the basis of their X values. The line is then calculated from the mean values of each group (Curran and Hay, 1986; Wald, 1940).

In Situ Measurements

A total of 216 reference sites were selected and field visited during the weeks after the scene registration of 29 August

TABLE 1. RANGES OF FOREST PARAMETER VALUES MEASURED IN (1) THE 65 SITES FROM 1989 USED FOR ANALYSIS OF THE TERRAIN EFFECT AND DEVELOPMENT OF CORRECTION MODELS, AND (2) THE 40 Verification Sites from 1989 (THE VERIFICATION SET FROM 1985 HAD APPROXIMATELY THE SAME RANGES).

Forest Parameter	Range development sites	Range verification sites
Slope gradient	0–28°	0–25°
Age	70–100 yrs	70–100 yrs
Defoliation (needle loss)	13–37%	15–34%
Hardwood component	0–6%	0–21%
Pine component	0–12%	0–22%
Timber volume	160–260 m^3/ha	120–275 m^3/ha
Density	170–270 st/ha	140–280 st/ha

1989. Out of these, 80 were located on inclined surfaces and were used in the terrain analyses, together with 25 near-horizontal sites. Several authors studying terrain effects have attributed high levels of variability in observed radiances to canopy inhomogeneity within the test sites (Cavayas, 1987; Teillet *et al.*, 1982; Hall-Könyves, 1987). Therefore, homogeneity was strongly emphasized in the selection of reference sites. Only relatively small stands (0.6 to 1.2 hectares) were sufficiently homogeneous. All such areas covered by the aerial photography were selected for study (216 sites). The measured site characteristics from 1989 were assumed to be valid also for the 1985 data, except for the defoliation which was assessed for both years. The canopy parameters measured in the field were age, basal area, mean height, timber volume, site quality, and understory. These were measured in three to six plots per site, the number of plots depending on the site homogeneity. A three-plot site was divided into three equally sized sections, and the plots were located in the centers of these sections. Each plot was 0.03 ha in size. The slope and aspect were determined using clinometer and compass. Two measurements were carried out for each slope in the test site. Some sites had slightly diverging slope degrees or aspects in two or three site parts, and in these sites four or six measurements were carried out. The resulting site slope gradients ranged between 0° and 28°, and the aspects were evenly distributed in all directions. Species composition, stems per hectare, and mean stand defoliation (needle loss) were determined using color infrared aerial photography at a scale of 1:6,000 acquired on 21 September 1989, and at a scale of 1:10,000 acquired on 27 July 1985. Two separated strips of photography were flown across the 300-km^2 study area in 1989, covering one fifth of the area. Two strips were flown in 1985, covering one third of the area because the scale was smaller. Table 1 shows the ranges of the parameters measured in the reference sites. The defoliation assessment was carried out according to methods described by Ekstrand (1994b). All clearly distinguishable trees (40 percent) in the sites were categorized into 20 percent defoliation classes (0 to 20 percent, 21 to 40 percent, etc.) using the aerial photography. The mean spruce needle loss for each site was calculated by summing the number of trees in each category (e.g., 21 to 40 percent) and multiplying them with the class midpoint (e.g., 30 percent). The resulting values for the five categories were added up and divided by the total number of spruce trees, thus calculating a mean needle loss for the site, presented in percent.

The air photo estimation was calibrated to the field estimation of the Swedish National Forest Survey using 200 field-estimated control trees. Another 100 trees were used for accuracy validation. The air photo assessed mean needle loss for 100 trees was very close to the field estimate, i.e., 32.5 percent compared to 29.9 percent (Ekstrand 1994b).

The test sites were delineated in the aerial photography and subsequently the borders were transferred to the satellite imagery. Two methods were considered for this procedure. The first was to identify the test site in the forest map, to extract the national grid coordinates for the center point, and then to transmit them to the satellite imagery. However, exact map identification of the air-photo-delineated test sites were sometimes impossible to carry out. Furthermore, the need for homogeneity within the sites made it unfeasible to maintain a specific site outline, for example, a square, which is a prerequisite if the coordinates of the center or corner points are to be used for delineation in the satellite imagery. This method also made it difficult to manually correct for the geometric displacement which locally may be as large as one pixel also in imagery that is geometrically corrected with high precision (RMSE < 0.5 pixels). The approach chosen in the present study was to visually identify the air-photo-delineated test sites in the enlarged satellite imagery. For sites in the middle of large old growth forest areas, this proved to be equally difficult, but, if small forest gaps or younger stands were located less than five pixels away from the site, the delineation using this method was more exact. After delineation in the satellite imagery, the border pixels were excluded. The presence of large, open surfaces close to the sites would affect the recorded site spectral radiance. Therefore, such sites were excluded from analysis.

Analysis

The mean reflectance was calculated for each reference site (6-17 pixels) and used in the terrain analyses. Sixty-five sites, out of which 15 were horizontal or near-horizontal (<3°), were used to develop empirical functions, based on the Landsat data from 1989. The functions were verified with the data from 28 September 1985 (the same 65 sites) and 12 September (22 out of 65 sites). A larger number of sites for the 12 September scene would have been beneficial but, because it was a neighboring scene with sites only in the overlap area, only 22 sites could be found. The remaining 30 inclined sites were used in the verification of the final damage assessment together with ten sites located on near-horizontal surfaces.

The topographic effect was plotted for the TM spectral bands of August 1989 (Figure 2). Linear and non-linear regression analyses of cos i versus spectral bands were performed using Statgraphics software. Non-linear functions were determined using least-squares matching of a predefined function type (in this case, $L(\lambda) = a + b^{(c \cos i)}$, where a, b, and c are constants that are iteratively tested). Topographic correction equations based on these functions and on Minnaert functions were analyzed. The reference site cos i values used in these analyses were calculated from the field measured slope/aspects. In the final application of the developed correction functions employing digital elevation models, cos i values were calculated for each pixel from which a mean cos i for each stand was computed. The Minnaert values were initially computed by solving Equation 6 for k. Spectral radiance values for 10°, 20°, and 30° slopes in different directions were calculated from the non-linear regression line of spruce radiance versus cos i. These were, together with the radiance of horizontal surfaces, used to solve Equation 6 for k, for the 10°, 20°, and 30° slopes. The Minnaert constant (k) was calculated using one cos i value at a time. The radiance of horizontal surfaces was determined by calculating the mean of the observed radiance from 20 homogeneous, horizontal sites. As it became clear that the Minnaert constants changed closely with cos i for different aspects, constants changing with cos i were tested (see Results). The capability of ratios to eliminate topographic effects was ana-

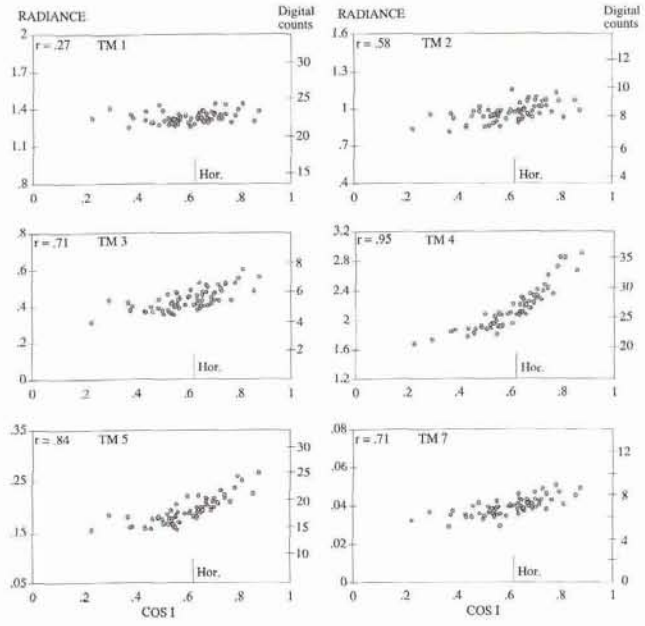

Figure 2. Landsat TM band radiances (mW/(sr cm² µm)) from 29 August, 1989, versus cosine of the incidence angle. Sixty-five test sites with slopes of 0 to 28° and aspects evenly distributed in all directions. All correlation coefficients but TM band 1 were calculated for non-linear relationships.

lyzed by plotting ratio values for the test sites against cos *i*. Ratio values were calculated from spectral radiance values corrected for additive atmospheric effects.

Partial correlation analysis was employed to compare the spectral significance of changes in topography with the significance of varying defoliation, species composition, age, and density. The partial correlation coefficient measures the relationship between two variables while controlling for possible effects of other variables. These effects are controlled by removing the linear relationship with the other variables before calculating the correlation coefficients between the two variables of interest. Only linear functions were considered. This analysis was carried out on the verification set of 40 unused test sites, where variations in the forest parameters were allowed (Table 1).

In the final step, the chosen topographic correction function, verified on the two additional scenes from 1985, was incorporated in the earlier developed model (Ekstrand 1994a). This model was originally designed to modify radiance values based on age, density, and species variations taken from forest maps (see Results). A forest damage assessment was performed for which the classification accuracy using field measured slope/aspect data were compared to the accuracy of an assessment using slope/aspect derived from the digital elevation model (DEM).

Integration of the Elevation Model

A digital elevation model with a 50-metre grid spacing was purchased from the Swedish Land Survey and converted to raster imagery. The height accuracy is ±2.5 metres but, in terrain characterized by steep hillocks, errors of ±5 metres may occur. With these accuracies, uncertainties of 10° to 20° may occur but, because stand mean values were used, the errors were strongly reduced. The elevation model covered 300 km² (identical to the study area). In the rasterization of the DEM grid points, the altitude values were generalized from decimetres to metres. The data were resampled to 25-metre pixels to geometrically match the Landsat TM imagery and the digitized forest maps. The procedure reduces the influence of a high elevation value, extending across the border to what is actually horizontal ground when calculating slopes. It also improves the geometric location of the calculated slopes in sharp terrain. The transformation to 25-metre pixels was carried out by zooming the original image with a factor of two. Then one column and one row were removed from the upper left of the image in order to fit the center of each 2- by 2-pixel block to the position of the original grid point. The result is similar to a resampling using the nearest-neighbor method. After this procedure, the slope and aspect images were calculated using the methods described below. In a test employing 20 sites, the mean deviation for the calculated site slope compared to the observed slope was 3.2°. This test also showed that 25-metre data resampled from the 50-metre data performed better than the 50-metre data itself (mean dev. 5.3°). The slope and aspect derived using this resample method may be somewhat different for single pixels compared to slope/aspects derived from a resample based on cubic convolution. The latter method smooths the altitude differences between pixels and therefore possibly also reduces the slope values in sharp terrain.

Two methods to calculate slope and aspect were tested. One of them computes the aspect at a point as the orientation of the plane formed by the vector connecting the left and right neighbors and the vector connecting the upper and lower neighbors of the pixel. The aspect is the angle between north (top of image) and the projection of the normal vector of this plane onto the horizontal plane The other method computes the mean of the three vectors connecting the three left neighbors with the three right neighbors, as well as the mean of the three vectors connecting the three upper neighbors with the three lower neighbors. The latter methods accounts for a larger part of the terrain features in the 3 by 3 matrix. The errors produced by the two-vector calculation of slope/aspect are likely to be comparatively large. However, the difference between the methods can be assumed to be reduced by the choice of standwise assessment instead of pixelwise. From the slope and aspect images, a mean value (cos *i*) is calculated for each stand, based on the cos *i* values of the pixels within the stand. This way, the terrain features of "diagonal" pixels influence the result also with the two-vector method.

Results and Discussion

Spectral Effect of Topography

The order of spectral significance among the stand parameters was determined by partial correlation analysis performed on the verification set (Table 2). The terrain factor, expressed

TABLE 2. ORDER OF SPECTRAL SIGNIFICANCE AMONG COMPARTMENT PARAMETERS. PARTIAL CORRELATION ANALYSIS WITH TM BAND 4 AS DEPENDENT VARIABLE.

Independent variables	Partial correlation (r)	Significance value
Incidence angle	−0.78	0.000
Defoliation	−0.70	0.000
Hardwood component	0.52	0.000
Age	−0.13	0.475 not sign.
Pine component	0.04	0.701 not sign.
Stems/hectare	0.06	0.641 not sign.
Timber volume	0.02	0.824 not sign.

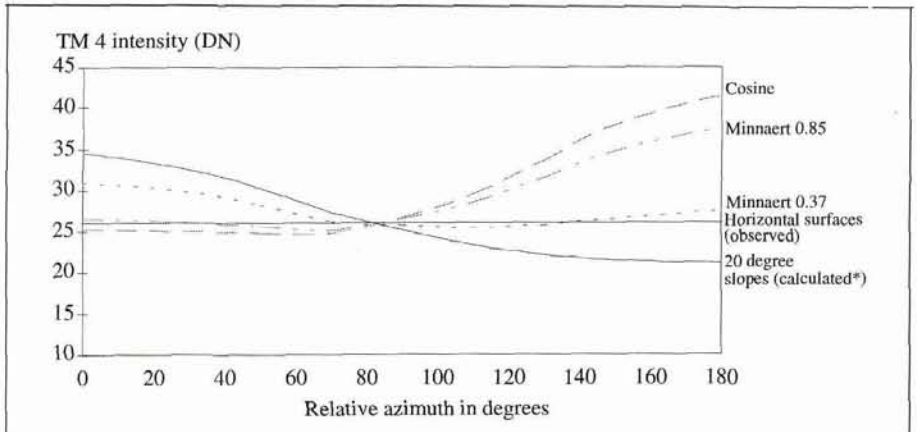

Figure 3. The effect of earlier proposed cosine and Minnaert corrections on the TM band 4 intensity of 20° spruce slopes (relative azimuth is the difference between site aspect and sun azimuth).

as incidence angle, had the strongest influence on TM band 4, followed by defoliation and hardwood component. It must be noted that the partial correlation analysis considered only linear functions. Because incidence angle has a non-linear spectral response in the near-infrared region, the influence of this variable is underestimated when computing linear partial correlation coefficents. The dominance of incidence angle would have been even greater if non-linear functions could have been included in the analysis. In the interpretation of Table 2, it is important to be aware of the ranges of the different forest parameters, e.g., 15 to 34 percent defoliation, 120 to 275 m^3/ha. These are presented in Table 1. In general, the sites analyzed included 70- to 100-year-old spruce forest, with a density ranging from moderately sparse to dense, containing minority fractions of pine and hardwood, and located in flat to fairly steep terrain. The defoliation levels ranged from healthy to moderate. The stand parameter ranges are rather narrow. Nevertheless, this is the dominating type of mature forest in northern Europe.

The spectral effect of topography in spruce forest, as recorded on 29 August 1989, is presented in Figure 2. The effect is very pronounced in TM bands 4 and 5, in which both display a clear non-linear, and therefore non-Lambertian, response to an increasing cosine of the incidence angle. For TM bands 2, 3, and 7, the non-linearity is not as evident, although they exhibit a statistically significant relationship with topography. TM band 1 is the only band where topography has no clear effect. Cos i = 0 in Figure 2 is the boundary where northern slopes become shadowed, while cos i = 1 corresponds to southern slopes perpendicular to the sun.

Based on the non-linear regression line of cos i versus TM band 4, which is the spectral band to be used in the damage assessment (Ekstrand, 1994a), the radiances of 10°, 20°, and 30° slopes with different aspects were calculated. As expected, the correction of these radiance values for topography using the Lambertian cosine correction (Equation 3) yields acceptable results for south-facing slopes, while north-facing slopes are severely over-corrected, resulting in a reversed topographic effect, stronger than in the uncorrected data. This is shown for 20° slopes in Figure 3. In order to examine whether or not Minnaert constants previously developed for other tree species would also accommodate Norway spruce, the near-infrared Minnaert constant (Equation 5) for Ponderosa pine (0.37, Smith *et al.*, 1980) was employed. Again, 10°, 20°, and 30° slopes with different aspects were corrected. The results were better than for the Lambertian cosine correction, although the correction for southern slopes was not sufficient. For a 20° slope with a 10° relative azimuth (relative to the sun), the resulting correction factor was 0.86, while it should have been 0.75 to reach the level of known horizontal spruce surfaces. Using a Minnaert constant high enough to yield adequate corrections for southern slopes (k = 0.85) gave, on the other hand, poor results for the northern slopes (Figure 3). Minnaert constants earlier developed for Douglas fir (k = 0.96, Teillet *et al.*, 1982) and Lodgepole pine (k = 0.23, Teillet *et al.*, 1982) were also tested, but they did not improve the results. No single Minnaert constant resulted in accurate corrections for all slope/aspects. This lead to the conclusion that new Minnaert constants should be calculated for Norway spruce. This is in accordance with previous works referred to above. Furthermore, different corrections should be used for different values of cos i, something that was briefly discussed by Teillet *et al.* (1982) in the examination of Douglas fir and Lodgepole pine.

The following analysis aimed to compute new Minnaert values for Norway spruce. For several of the spectral bands, the Minnaert coefficients calculated by solving Equation 6 for k followed the change in cos i rather closely. Therefore, functions that allowed k to change according to the calculated k values for different cos i were tested iteratively. The corrections were applied to the spectral radiance values for the 10°, 20°, and 30° slopes in different directions (i.e., 10°, 20°, 30°, ..., 180° relative azimuth to the sun). The radiance values for these slopes were calculated from the non-linear regression line of the observed spruce radiance versus cos i (Figure 2). For TM band 4, a correction residual of 0.02 mW/(sr cm^2 μm) was accepted because this is the approximate effect of 1 percent needle loss in TM band 4 for the scenes studied (Ekstrand, 1994a). The function that gave the best result for all tested slope/aspects was chosen. During these computations, it was observed that the main effect of the slope factor in the numerator and denominator of Equation 5 (cos e and $\cos^k e$) was a constraint in the correction for northern slopes. For example, for a 20° slope with a 170° relative azimuth (relative to the sun position) and a k value of 0.30, the correction factor would be 1.16 with cos e and $\cos^k e$ in the function and 1.22 without. For a similar slope with 10° relative azimuth (almost facing the sun) and a k value of 0.90 (which was more appropriate for southern spruce slopes), the correction factor would be 0.75 with cos e and $\cos^k e$ in the function and 0.75 without. The constraint in the correction for northern slopes is not desirable if the k value is allowed to *change*, which was a necessity if accurate corrections were to be accomplished. This is because the change (in k) in itself accounts for the needed constraint in correc-

TABLE 3. MINNAERT CONSTANTS FOR THE TM SPECTRAL BANDS, TO BE EMPLOYED IN EQUATION 7, AND THE EMPIRICAL FUNCTIONS WHICH ARE BASED ON THE RELATIONSHIPS BETWEEN EACH SPECTRAL BAND AND THE COSINE OF THE INCIDENCE ANGLE.

Spectral band	Minnaert constant	Empirical function
TM 1		No clear topographic effect observed
TM 2	0.34 cos *i*	$L_H = L_T\,(0.712+0.823^{1.82\cos z})/(0.712+0.823^{1.82\cos i})$
TM 3	0.56 (rel. azimuths 0–90°), 0.36 (rel. azimuths 91–180°)	$L_H = L_T\,(0.224+0.676^{2.10\cos z})/(0.224+0.676^{2.10\cos i})$
TM 4	1.04 cos *i* (rel. azi. 0–60°), 0.97 cos *i* (rel. azi. 61–180°)	$L_H = L_T\,(1.495+1.519^{3.05\cos z})/(1.495+1.519^{3.05\cos i})$
TM 5	0.94 cos *i*	$L_H = L_T\,(0.130+0.195^{2.56\cos z})/(0.130+0.195^{2.56\cos i})$
TM 7	0.50 (rel. azi. 0–90°) 0.30 (rel. azi. 91–180°)	$L_H = L_T\,(0.023+0.059^{1.91\cos z})/(0.023+0.059^{1.91\cos i})$

tions of northern slopes. Therefore, the slope factor was excluded from Equation 5, giving

$$L_H = L_T\,(\cos z/\cos i)^k. \quad (7)$$

The Minnaert value calculated for TM band 4 by resolving Equation 7 for k changed from 0.29 to 0.90 for cos i values of 0.30 to 0.85. A similar continuous change was found for all spectral bands except TM band 1. However, for TM bands 3 and 7, the range was so narrow that it was sufficient to use two different values, one for north-facing slopes and one for south-facing slopes. For TM bands 2, 4, and 5, a Minnaert constant changing with the cos i had to be applied. In doing so, the corrected radiance values from the regression lines in Figure 2 diverged from the known horizontal intensity with less than one digital count (Table 3). As mentioned, for TM band 4, residuals no larger than 0.25 digital counts, or 0.02 mW/(sr cm^2 μm), were accepted. The function is written

$$L_H = L_T\,(\cos z/\cos i)^{r\cos i}, \quad (8)$$

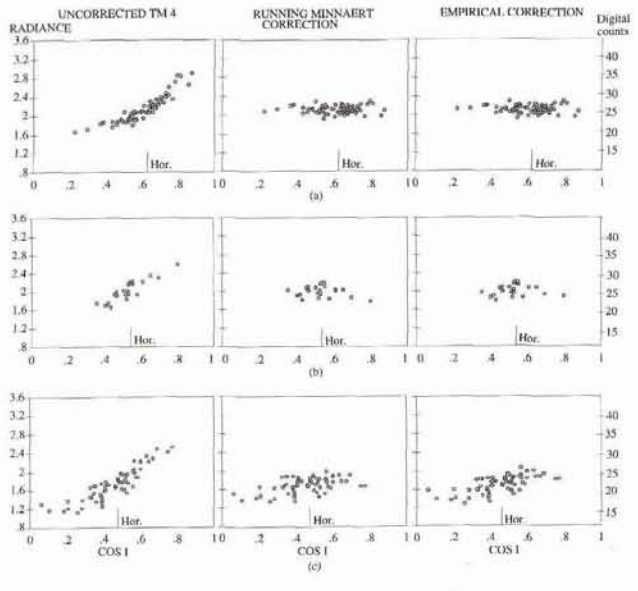

Figure 4. The correction efficiency of the "running Minnaert" and the empirical function, on TM band 4 radiance (mW/(sr cm^2 μm)). (a) 29 August 1989, 65 sites. (b) 12 September 1985, 22 sites. (c) 28 September 1985, 65 sites. The slightly different relationship between digital counts and radiance in (a) compared to (b) and (c) depends on differences in the radiometric correction of system corrected and geometrically corrected data, at the Swedish distributor SSC Satellitbild, Kiruna.

where r for TM band 4 = 1.04 for relative azimuths from 0 to 60°, and = 0.97 for relative azimuths from 61 to 180° (relative azimuth is the difference between the site aspect and the sun azimuth). Thus, the Minnaert constant, k, is replaced by (r cos i). The difference in correction effect between the two r values, 1.04 and 0.97, is small. For other applications it may suffice to apply an r value of 1.0. However, this results in a slight undercorrection for southern slopes and an overcorrection for northern slopes, in the data set examined. The error is comparable to the spectral effect of 1 to 2 percent defoliation; therefore, the model with two r values was chosen here. Figure 4 shows that the relationship between spectral radiance and topography was removed or strongly reduced.

A drawback with this function is that the correction factor slowly decreases for cos i values below 0.2 and becomes insufficient close to 0. Below 0, the function is not applicable (i.e., for slopes in shadow). Still, cos i values lower than 0.2 occur comparatively seldom for scenes with sun elevations above 25°, and, if they do, they are not likely to be vegetated by spruce forest.

An alternative empirical correction function can be formulated by applying the non-linear regression lines for TM bands 2 to 7 versus cos i (Figure 2) to the general form of Equation 8. For TM band 4 the correction is then accomplished by

$$L_H = L_T\,(1.495+1.519^{3.05\cos z})/(1.495+1.519^{3.05\cos i}). \quad (9)$$

The resulting function for each band is found in Table 3. These functions gave corrections as accurate as the "running Minnaert" constants for the scenes from 29 August 1989 and 12 September 1985. For the scene from 28 September 1985, with very low sun elevation (28°), the running Minnaert correction was slightly better. The corrections of TM band 4 are presented in Figure 4. The empirical function (Equation 9) is applicable for all cos i values, although it must be stressed that slopes in shadow (cos $i < 0$) have not been examined here.

A possible reason for part of the increased variability in the 1985 data (Figure 4) is the registration of 1985 data to 1989 data. The resampling was performed with a root-mean-square error of less than 0.5 pixels, but in some parts of the imagery the displacement was still one pixel large. This problem is hard to avoid with existing resampling software. Another factor that may have increased the variability in the two data sets from 1985 (Figure 4) is the fact that the test sites were assigned the same forest parameter values (for instance, species composition) in 1985 as in 1989. No management actions were carried out in the sites between 1985 and 1989, and no other changes were recorded during the field visits, but the possibility of small changes in the canopy or the understory cannot be excluded.

In the data from 12 September 1985, a slight undercorrection can be observed (Figure 4). This may imply that not only is the relationship cos z/cos i important, but also that

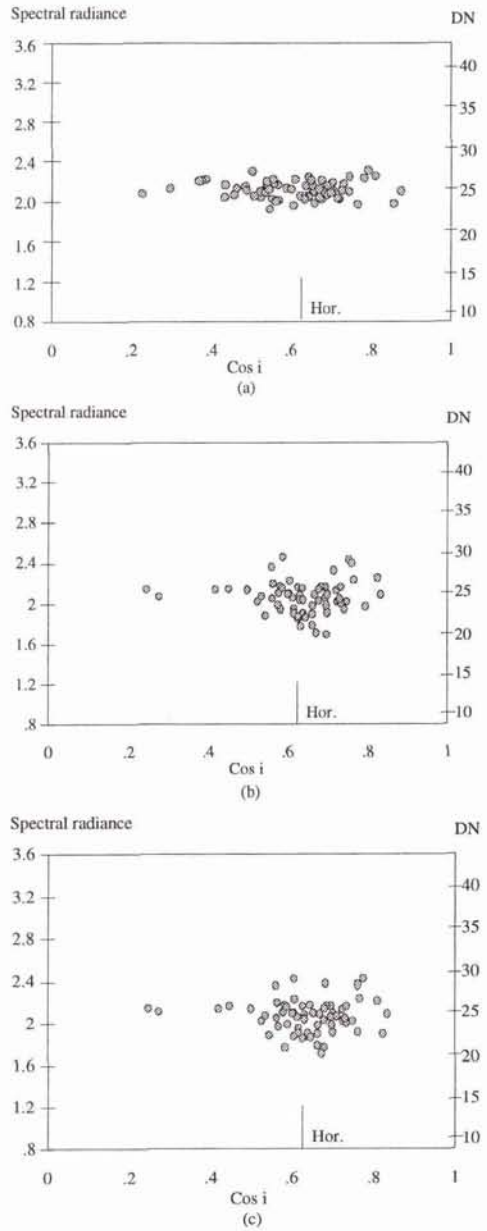

Figure 5. TM band 4 spectral radiance (mW/(sr cm² m)) corrected using the running Minnaert constant. (a) *In situ* measured slope/aspects. Slope/aspects computed from the DEM using (b) four neighbors and (c) eight neighbors.

the *size* of cos *z* is important. Unfortunately, the number of sites in the image from 28 September 1985 is too low to support this theory. Part of the cause may also lie in the observation geometry. The 28 September image was of a neighboring scene and the study area was observed away from the sun in this scene, while it was located towards the sun in the 1989 scene. The reason for the low number of sites for that Landsat TM recording is that sites were located only in the overlap area between the two scenes.

Apart from these potential error sources, it should be mentioned that the development set from 1989 contained only a few sites with cos *i* values below 0.4, while the number of sites in that range was high in the imagery from 12 September 1985. It is possible that the models should be slightly modified for sites with cos *i* values below 0.4.

The slope and aspect values used to calculate cos *i* for Figures 3 and 4 were measured in the field. Consequently, the results show the capability of the terrain corrections if nearly exact slope and aspect values are used as input. Computing slope and aspect from DEM data introduces the error sources associated with the resolution of the DEM; in this case, a 50-metre grid spacing in *x* and *y*, with a maximum error of ± 2.5 metres in *z* (although occasional errors of ± 5 metres are accepted in the terrain type examined). For instance, sharp terrain features between the 50-metre points will be disregarded. The effect of the errors introduced with the elevation model is presented for TM band 4 in Figure 5. The correction function removes the topographic effect in TM band 4 for 85 to 90 percent of the sites, with residuals of 1.5 digital counts or less (residuals of DEM correction minus *in situ* correction). For 10 to 15 percent of the sites, the correction residuals are large, here defined as 3.0 digital counts or more, due to deficient DEM slope/aspects. The largest residuals are 4 to 5 digital counts. This may be compared with the total topographic effect for the cos *i* range of the 1989 sites examined here; approximately 15 digital counts, or 1.3 mW/(sr cm² μm). Similar results were obtained for the other spectral bands and for the 1985 scenes. Two ways of computing slope/aspect from the DEM were tested. Figure 5b illustrates the method using four of the neighbors, omitting terrain features in the diagonal pixels. Figure 5c presents the results derived using the method that calculates a mean of the three vectors connecting the three left neighbors with the three right neighbors, as well as the mean of the three vectors connecting the three upper neighbors with the three lower neighbors. In this way, terrain features in all eight neighbors influence the slope/aspect of the center pixel. The correction results of the two methods are very similar. This can partly be attributed to the fact that standwise, not pixelwise, correction was employed. The mean cos *i* based on all pixels within the stand was calculated, and the correction was applied to the TM 4 stand spectral radiance. Hence, terrain features in "diagonal" pixels were accounted for also in the four-neighbor method. Furthermore, the resampling method results in blocks where four pixels have identical altitude values. This further decreased the differences between the four-neighbor and eight-neighbor methods. However, the error due to one-metre rounding is more influential in the four-neighbor method.

As mentioned, several ratio indices have earlier been used for forest damage assessment. These include TM bands 4/2, 4/3, 5/4 and the Normalized Difference Vegetation Index (NDVI, TM bands $(4 - 3)/(4 + 3)$). Their capacity to reduce terrain effects has been studied by authors referred to above. For comparative reasons, this capacity was examined also for the data used here. The results show that, when path radiance has been removed, all ratio indices except TM 4/2 corrected very well for terrain effects. The corrections achieved by TM 5/4 and NDVI are presented in Figure 6. The poor performance of TM 4/2 (and TM 4/1 which was studied in a follow-up test) suggests that blue and green spectral bands have such a low response to topography in spruce forest that they should not be used in ratios together with highly sensitive bands, if the purpose is to reduce topographic effects. Nevertheless, the good results for the other ratio indices support the conclusions of Rock *et al.* (1986) and Vogelmann (1990) that they are suitable for damage assessment in areas exhibiting both chlorosis (yellowing) and defoliation.

In Sweden chlorosis, defined as the persistent yellowing of sun-exposed needles, seldom occurs. The sole damage symptom is defoliation, for which a single-band estimation function gives superior results (Ekstrand, 1994a). Therefore, single-band topographic corrections such as the two alternatives presented here must be employed. Because of its

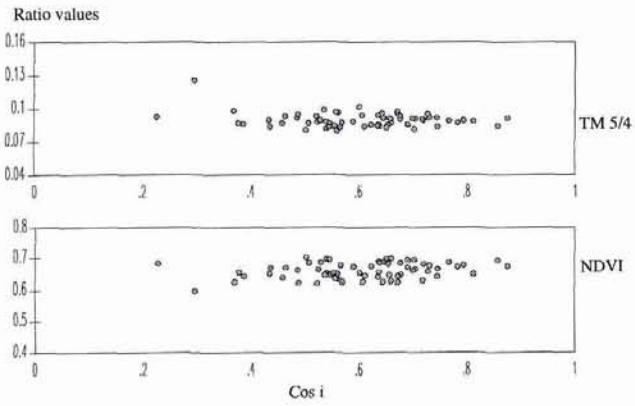

Figure 6. TM 5/4 and TM (4 − 3)/(4 + 3) known as the Normalized Difference Vegetation Index (NDVI) versus cosine of the incidence angle. The ratios are based on spectral radiance values.

slightly better performance for the Landsat TM imagery examined here, the "running Minnaert" function (Equation 8) was chosen for the damage assessment application. However, both of the spruce topographic correction models presented provide strongly improved results for satellite scenes with medium and low solar elevations.

Defoliation Assessment Model

The purpose of the earlier developed forest damage model (Ekstrand, 1994a) was to account for spectral variations caused by variability in the stand characteristics. This is accomplished by modifying the TM band 4 radiance based on information about the forest characteristics in each compartment, extracted from digitized forest maps. For damage assessment, age may be accounted for by simply excluding stands younger than 70 years from defoliation assessment. Spruce forest younger than that is seldom suffering from forest decline symptoms in the region and, more importantly, the age spectral response is stable from 70 years and up. For the density factor it is sufficient to exclude very sparse and very dense compartments (below 120 m^3/ha and above 310 m^3/ha) composing only 6 percent of the spruce forest area in the region (Ekstrand, 1994a). The remaining factor, species composition, has to be corrected for in a more detailed way. Based on the spectral response of pine and hardwood minority fractions, a simple correction model for forest on level ground was developed (Ekstrand, 1994a): i.e.,

$$L_{c(0.83)} = L_{(0.83)} - 0.0066P - 0.0156H, \quad (10)$$

where $L_{c(0.83)}$ is the corrected compartment radiance of TM band 4, $L_{(0.83)}$ is the original compartment radiance, P is the pine component in percent, and H is the hardwood component in percent. The constants express the spectral effects of one percent pine and one percent hardwood, respectively (Ekstrand, 1994a). Incorporating the topography correction function (Equation 8) in Equation 10 gives the final correction model expressed by

$$L_{c(0.83)} = L_{(0.83)}((\cos z/\cos i)^{r \cos i}) - 0.0066\ P - 0.0156\ H. \quad (11)$$

The defoliation (needle loss in percent) is then estimated by the inverted regression of TM band 4 on needle loss (Ekstrand 1994a): i.e.,

$$D = (L_{c(0.83)} - 2.4185)/-0.0189. \quad (12)$$

The verification of Equations 11 and 12 was accomplished by plotting predicted versus observed defoliation and determining the classification accuracy. The resulting values of percent needle loss for each stand were divided into two classes: healthy and slightly defoliated as one class (0 to 25 percent mean needle loss), and moderately defoliated as the other (>25 percent mean needle loss). Forty unused reference sites were employed in the verification set from 28 August 1989. The variation ranges of the forest parameters in the verification set are presented in Table 1. The verification was carried out for two cases.

In the first case, the information on stand parameters was extracted from the digitized forest maps, and the terrain data from the field measurements. Consequently, this case shows the accuracy when "true" terrain data were used, involving no error sources from the DEM. The relationship between estimated and observed defoliation was relatively strong (r = 0.71). A division of the defoliation into the two defined classes, below and above 25 percent mean needle loss, gave a classification accuracy of 78 percent. It must be stressed that this figure is affected by an error source that would not appear in operational inventories. Because most of the study sites covered only part of a larger compartment, the stand parameter values of the map, estimated for the entire compartment, were not always exact for the specific part covered by the study site. In operative inventories, the entire compartment would be assessed and the accuracy would lie between 78 percent and 82 percent, depending on the quality of the forest maps. Eighty-two percent is the accuracy derived when the stand parameter information of the forest map is void of errors. Compared to the accuracy on horizontal surfaces, 80 to 85 percent (Ekstrand, 1994a), the decrease in accuracy is small, indicating a successful topographic correction.

In the second case, the terrain information was taken from the digital elevation model. Comparison of Figures 7a and 7b gives an idea of the errors introduced by the elevation model. The classification accuracy decreased from 78 to 82 percent to 72 to 75 percent.

The model was also verified on Landsat TM data from 12 September 1985, relatively calibrated to the 1989 scene using the method described above. Only one strip of aerial color infrared photography (used for the reference defoliation assessment) flown within the study area was covered by the scene from 12 September 1985. Twenty-two reference sites with 80 to 100 percent spruce could be located within this strip. The defoliation classification accuracy was 71 percent. The somewhat lower accuracy compared to the data set from 1989 may be attributed to the inter-scene radiometric and geometric calibration, which is never absolutely correct, but also to the reference defoliation assessment, performed using aerial CIR-photography at a scale of 1:10,000. With this scale,

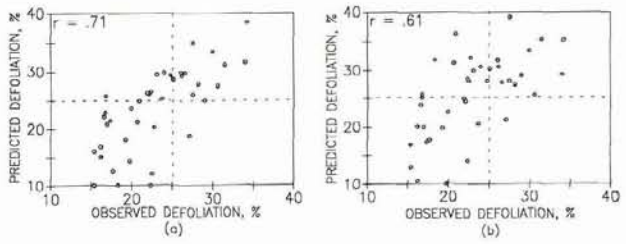

Figure 7. Predicted versus observed defoliation when the topography is accounted for using the running Minnaert model, and canopy variations using forest maps. (a) *In situ* measured terrain characteristics. (b) DEM derived terrain characteristics.

the defoliation estimation is slightly more uncertain than with the 1:6,000-scale photography which was used for the 1989 reference assessment.

The three main error sources in operative Swedish inventories will be the relatively coarse division of species composition in the existing forest maps (Ekstrand, 1994a), the 50-metre resolution of the DEM together with the computation of slope/aspect, and the inter-scene radiometric calibration. Species composition is categorized into tenths and not into percent in the forest map surveys. Tests in the study area showed that this error source, together with some misclassification by the field surveyor, caused a mean deviation from the correct percentage of ± 5.5 percent. In the case of hardwood, this would yield a defoliation error of 4 to 5 percent needle loss. For pine, the defoliation error would be 1 to 2 percent needle loss. The study area is one of the more difficult in Sweden, which was one of the reasons for choosing it. The forest compartments are small and inhomogeneous, and the terrain is composed of steep hillocks. Thus, the accuracy of the forest maps and the DEM is comparatively low. The effect of the errors originating from the forest maps is relatively small, but influences the majority of the compartments. It creates an increase in the standard deviation of estimated defoliation of 4 to 5 percent needle loss, but, with only two classes, the increase in number of misclassified stands is relatively low. Contrary to this, the DEM effect is large for 10 to 15 percent of the compartments, but negligible for the rest. For these 10 to 15 percent of the compartments, the resulting error is equivalent to 15 percent needle loss or more, and consequently most of them are misclassified.

In spite of the complex conditions of the area, the acquired defoliation accuracies were acceptable (72 to 75 percent). In areas with flat or gently undulating terrain and consequently more homogeneous forest canopy, the accuracy will be approximately 80 percent (Ekstrand, 1994a). To avoid the uncertainties of inter-scene calibrations, it is recommended that a limited air-photo-based reference damage assessment be carried out in new inventories.

Conclusions

The topographic effect in Norway spruce forest as measured by Landsat TM has been described in this paper. The effect was found to be non-Lambertian for the examined medium and low solar elevations. The Minnaert function earlier proposed for other forest types was found to be inadequate when using one fixed Minnaert constant for each spectral band. Two correction models were developed, one based on a Minnaert constant changing with the cosine of the incidence angle, and one based on an empirical function. Both models produced adequate corrections for the data analyzed, although the empirical correction performed better for nearly shadowed northern slopes. The errors introduced by the DEM, together with the computation of slope/aspect, were sometimes large, but they affected only a limited percentage of the slopes and therefore did not hamper the applicability.

The basic objective was to develop methods to account for topographic effects and canopy variations in forest damage assessment. Incorporation of the terrain correction function in an earlier developed model accounting for forest canopy inhomogeneities gave satisfactory results. It seems possible to separate *healthy to slightly* defoliated spruce forest from *moderately* defoliated forest with an accuracy of 72 to 75 percent in very rugged terrain and with approximately 80 percent accuracy in flat or gently undulating terrain. These results constitute an improvement over the earlier documented Landsat TM capability to detect severely damaged or dying forest. Regional satellite based defoliation assessments may thus be used to identify stands where vitalization measures are needed in order to prevent production losses and the evolving of severe, irreversible damage.

Acknowledgments

This research was supported by the Swedish Environmental Research Institute and the Swedish Board for Space Activities. Many thanks to Prof. Friedrich Quiel for valuable comments on this paper and constructive suggestions during the course of the project.

References

Bukata, R.P., J.E. Bruton, and J.H. Jerome, 1983. Use of chromaticity in remote measurements of water quality, *Remote Sensing of Environment*, 13:161–177.

Cavayas, F., 1987. Modelling and correction of topographic effect using multi-temporal satellite images, *Canadian Journal of Remote Sensing*, 13(2):49–67.

Chavez, P S., Jr., and W.B. Mitchell, 1977. Computer enhancement techniques of Landsat MSS digital images for land use/land cover assessments, *Proceedings of the 6th Annual Remote Sensing of Earth Resources Conference*, 29-31 March, pp. 259–276.

Ciolkosz, D.L., and T. Zawila-Niedzwiecki, 1990. Remotely sensed data and limitations of forest productivity in Poland, *Nature & Resources*, 26:41–44.

Civco, D.L., 1989. Topographic normalization of Landsat Thematic Mapper digital imagery, *Photogrammetric Engineering & Remote Sensing*, 55(9):1303–1309.

Colby, J., 1991. Topographic normalization in rugged terrain, *Photogrammetric Engineering & Remote Sensing*, 57(5):531–537.

Curran, P.J., and A.M. Hay, 1986. The importance of measurement error for certain procedures in remote sensing at optical wavelengths, *Photogrammetric Engineering & Remote Sensing*, 52(2): 229–241.

Ekstrand, S., 1990. Detection of moderate damage on Norway spruce using Landsat TM and digital stand data, *IEEE Transactions on Geoscience and Remote Sensing*, 28(4):685–692.

———, 1994a. Assessment of forest damage with Landsat TM: Correction for varying forest compartment characteristics assessment of forest damage, *Remote Sensing of Environment*, 47:291–302.

———, 1994b. Close range forest defoliation effects of traffic emissions assessed using aerial photography, *Science of the Total Environment*, 146/147:149–155.

Gordon, H.R., 1987. Calibration requirements and methodology for remote sensors viewing the ocean in the visible, *Remote Sensing of Environment*, 22:103–126.

Hall-Könyves, K., 1987. The topographic effect on Landsat data in gently undulating terrain in southern Sweden, *International Journal of Remote Sensing*, 8(2):157–168.

Holben, B.N., and C.O. Justice, 1980. The topographic effect on spectral response from nadir-pointing sensors, *Photogrammetric Engineering & Remote Sensing*, 46(9):1191–1200.

Jones, A.R., J.J. Settle, and B.K. Wyatt, 1988. Use of digital terrain data in the interpretation of SPOT-1 HRV multispectral imagery, *International Journal of Remote Sensing*, 9(4):669–682.

Kawata, Y., S. Ueno, and T. Kusaka, 1988. Radiometric correction for atmospheric and topographic effects on Landsat MSS images, *International Journal of Remote Sensing*, 9(4):729–748.

Kimes, D.S., and J.A. Kirchner, 1981. Modeling the effects of various radiant transfers in mountainous terrain on sensor response, *IEEE Transactions on Geoscience and Remote Sensing*, 19(2): 100–108.

Koch, B., U. Ammer, T. Schneider, and H. Wittmeier, 1990. Spectroradiometer measurements in the laboratory and in the field to analyse the influence of different damage symptoms on the reflection spectra of forest trees, *International Journal of Remote Sensing*, 11(7):1145–1163.

Kowalik, W.S., R.J.P. Lyon, and P. Switzer, 1983. The effects of addi-

tive radiance terms on ratios of Landsat data, *Photogrammetric Engineering & Remote Sensing*, 49(5):659–669.

Kriebel, K.T., 1976. On the variability of the reflected radiation field due to differing distributions of the radiation, *Remote Sensing of Environment*, 4:257–264.

Leprieur, C.E., J.M. Durand, and J.L. Peyron, 1988. Influence of topography on forest reflectance using Landsat Thematic Mapper and digital terrain data, *Photogrammetric Engineering & Remote Sensing*, 54(4):491–496.

Leckie, D.G., 1987. Factors affecting defoliation assessment using airborne multispectral scanner data, *Photogrammetric Engineering & Remote Sensing*, 53(12):1665–1674.

Minnaert, M., 1941. The reciprocity principle in lunar photometry, *Astrophysical Journal*, 93:403–410.

Olsson, H., 1993. Regression functions for multitemporal relative calibration of thematic mapper data over boreal forest, *Remote Sensing of Environment*, 46:89–102.

Proy, C., D. Tanré, and P.Y. Deschamps, 1989. Evaluation of topographic effects in remotely sensed data, *Remote Sensing of Environment*, 30:21–32.

Rock, B.N., J.E. Vogelmann, D.L. Williams, A.F. Vogelmann, and T. Hoshizaki, 1986. Remote detection of forest damage, *BioScience*, 36(7):439–445.

Rosengren, M., and S. Ekstrand, 1987. A method aiming at monitoring of large-area forest decline using satellite imagery, *Proceedings of the Seminar on Remote Sensing of Forest Decline Attributed to Air Pollution*, Laxenburg, Austria, 2:1–20.

Rowan, L.C., A.F.H. Goetz, and R.P. Ashley, 1977. Discrimination of hydrothermally altered and unaltered rocks in visible and near infrared multispectral images, *Geophysics*, 42(3):522–535.

Smith, J.A., T.L. Lin, and K.J. Ranson, 1980. The Lambertian assumption and Landsat data, *Photogrammetric Engineering & Remote Sensing*, 46(9):1183–1189.

Syrén, P., 1991. Forest Canopy reflectance as a function of solar elevation and forest parameters, *Proceedings of the Int. Geoscience and Remote Sensing Symposium (IGARSS'91)*, Espoo, Finland, 3-6 June, pp. 1537–1540.

Teillet, P.M., B. Guindon, and D.G. Goodeonugh, 1982. On the slope-aspect correction of multispectral scanner data, *Canadian Journal of Remote Sensing*, 8(2):84–106.

Thomson, A.G., and C. Jones, 1990. Effects of topography on radiance from upland vegetation in North Wales, *International Journal of Remote Sensing*, 11(5):829–840.

Tomppo, E., 1989. Comparisons of some classification methods in satellite image aided forest tax class estimation, *Proceedings of the 6th Scandinavian Conference on Image Analysis*, Oulu, Finland, 19-22 June, pp. 150–157.

Vogelmann, J.E., 1990. Comparison between two vegetation indices for measuring different types of forest damage in the north-eastern United States, *International Journal of Remote Sensing*, 11(12):2281–2297.

Vogelmann, J.E., and B.N. Rock, 1989. Use of Thematic Mapper data for the detection of forest damage caused by the pear thrips, *Remote Sensing of Environment*, 30:217–225.

Wald, A., 1940. The fitting of straight lines if both variables are subject to error, *Annals of Mathematical Statistics*, 11:162–186.

Westman, W.E., and C.V. Price, 1988. Detecting air pollution stress in southern California vegetation using Landsat Thematic Mapper band data, *Photogrammetric Engineering & Remote Sensing*, 54(9):1305–1311.

Woodham, R.J., and M.H. Gray, 1987. An analytical method for radiometric correction of satellite multispectral scanner data, *IEEE Transactions on Geoscience and Remote Sensing*, 25(3):258–271.

Yugui, Z., 1989. *Normalization of Landsat TM Imagery by Atmospheric Correction for Forest Scenes in Sweden*, Research Report, Remote Sensing Laboratory, Swedish University of Agricultural Sciences, Umeå, 28 p.

(Received 7 May 1993; revised and accepted 1 February 1994; revised 10 October 1994)